1 *Article*

2 # Furin prodomain ppFurin enhances SOCE through TRPC6 activation in

3 # breast cancer cells

4

5 **Jose J. López[1†], Geraldine Siegfried[2†], Carlos Cantonero[1], Jean Descarpentrie[2], Tarik Smani[3], Iker**

6 **Badiola[4], Simon Pernot[5], Serge Evrard[5], Juan A. Rosado[1‡] and Abdel-Majid Khatib[2, 3‡]**

7 ‡, † Equal Contribution

8

9 [1] Department of Physiology, University of Extremadura, Caceres, Spain; jjlopez@unex.es (J.J.L),
10 carloscantonero@unex.es (C.C.), jarosado@unex.es (J.A.R).
11 [2] Univ. Bordeaux, INSERM, LAMC, U1029, F-33600 Pessac, France; geraldine.siegfried@inserm.fr; (G.S)
12 descarpentrie.jean@gmail.com (J.D), majid.khatib@inserm.fr (AM. K)
13 [3] Department of Medical Physiology and Biophysics, University of Seville, Seville 41009, Spain; tasmani@us.es
14 (T.S.)
15 [4] Department of Cell Biology and Histology, Faculty of Medicine and Nursing, University of the Basque
16 Country, 48940 Leioa, Spain, iker.badiola@gmail.com (I.B)
17 [5] Bergonié Institute, Bordeaux, France; S.Evrard@bordeaux.unicancer.fr (S.E), s.pernot@bordeaux.unicancer.fr
18 (S.P)
19

20 * Correspondence: majid.khatib@inserm.fr (AM. K); and jarosado@unex.es (J. A.R);

22

23 **Abstract:**
24 The intracellular calcium concentration ($[Ca^{2+}]_i$) modulation plays a key role in the regulation of
25 cellular growth and survival in normal cells and failure of $[Ca^{2+}]_i$ homeostasis is involved in tumor
26 initiation and progression. Here we show that inhibition of Furin by its naturally occurring inhibitor
27 the prodomain ppFurin in the MDA-MB-231 breast cancer cells resulted in enhanced SOCE through
28 TRPC6 activation that associated reduced cells malignant phenotype. Expression of ppFurin in a
29 stable manner in MDA-MB-231 and the melanoma MDA-MB-435 cell lines inhibits Furin activity as
30 assessed by *in vitro* digestion assays. Accordingly, cell transfection experiments, revealed that the
31 ppFurin-expressing cells are unable to process adequately the PC substrates proVEGF-C and
32 proIGF-1R. Compared to MDA-MB-435 cells, expression of ppFurin in MDA-MB-231 significantly
33 induces Ca^{2+} entry which is impaired by silencing of TRPC6 expression. Analysis of TRPC6
34 activation revealed its up-regulated tyrosine phosphorylation in ppFurin-expressing MDA-MB-231
35 cells. The expression of ppFurin in MDA-MB-231 cells reduced their viability and ability to migrate
36 and enhanced their sensitization to the apoptosis inducer hydrogen peroxide. These findings
37 suggest that Furin inhibition by ppFurin may be a useful strategy to interfere with Ca^{2+} mobilization
38 leading to breast cancer cells malignant phenotype repression and reduction of their resistance to
39 treatments.

40 **Keywords:** Furin; ppFurin; Breast cancer; Calcium; SOCE; TRPC6; Viability; Migration.
41

42 ## 1. Introduction

43   After lung cancer, breast cancer is the second most common cancer worldwide; and the
44 incidence of this cancer is continually increasing and even though treatment of breast cancer has
45 improved in recent years more than 600,000 people still died from this disease every year [1]. Like
46 various cancers breast cancer directly involves changes in intracellular Ca^{2+} dynamics [2,3]. Such

variations are frequently associated with intensification of cancer-related processes, including cell proliferation, migration and/or escaping of cell apoptosis [2,3]. In breast cancer cells, the levels of Ca^{2+} can be increased by the influx of extracellular Ca^{2+} via the Ca^{2+} channels in the plasma membrane. In addition, the remodeling of Ca^{2+} homeostasis can be mediated by changes in the expression of these channels and Ca^{2+} pumps as well [4]. In many circumstances, changes in $[Ca^{2+}]_i$ are controlled by intracellular Ca^{2+} store mobilization and Ca^{2+} influx through hormones, growth factor receptors activation [2–4]. Interestingly, wide range of these secretory proteins are synthesized as inactive precursors that are converted to their bioactive forms at the general motif (K/R)-(X)n-(K/R)$\downarrow$, where n= 0, 2, 4 or 6 by Furin-like enzymes [5–8].

Furin, also known as PCSK3, is a proprotein convertase that belongs to a family of Ca^{2+}-dependent serine peptidases. Synthesized as a precursor protein (preppFurin), this enzyme requires autocleavage in the secretory pathway for its activation [5,9,10]. Following the removal of the "pre" signal peptide in the endoplasmic reticulum (ER), the remaining protein is than autocatalytically processed in the secretory pathway to generate the N-terminal ppFurin fragment and mature active Furin. N-terminal ppFurin fragment is associated with the enzyme functions as a potent inhibitor [5,9,10]. The presence of a C-terminal membrane binding domain [5,9,10] in the mature Furin allows this enzyme to cycle between the Golgi and plasma membrane and mediate the maturation of a strikingly varied set of proproteins. These include growth factors, receptors and differentiation factors, adhesion molecules and proteases, which have been associated with tumor initiation and different stages of tumor progression, angiogenesis, immune response and metastasis [5,6,11–14]. Based on various studies describing the activation of many proteins implicated in neoplasia by Furin, such as growth factors, their receptors, proteases and adhesion molecules, it was hypothesized that this protease may constitute a new potential target for cancer therapy [5,6,11–13]. Subsequently, comparative analysis of normal and tumor tissues derived from patients revealed altered expression levels of Furin in various types of cancers including breast cancer [5,15].

In this study, we aimed to characterize Ca^{2+} changes in response to Furin repression by ppFurin in MDA-MB-231 breast cancer cells, with a focus on investigating the relationship between Ca^{2+} concentration changes, TRPC6 activation and malignant phenotype repression by ppFurin. Our results indicate that ppFurin mediates Ca^{2+} influx by means of TRPC6 channels activation that associates with MDA-MB-231 cells viability and migration reduction and enhances sensitization to the apoptotic agent hydrogen peroxide. These studies provide new insights into the consequences of Furin activity on Ca^{2+} homeostasis in breast cancer cells.

2. Results

2.1. Furin activity is repressed by ppFurin in breast cancer cells

To investigate the role of Furin in the regulation of Ca^{2+} mobilization in breast cancer cells, MDA-MB231 were stably transfected with pIRES2-EGFP empty vector (Control) or containing ppFurin cDNA. For comparison, the melanoma cells MDA-MB435 were also transfected with pIRES2-EGFP empty vector (Control) or containing ppFurin. Using an *in vitro* enzymatic digestion assay [16,17] and the universal proprotein convertases (PCs) substrate: the fluorogenic peptide pERTKR-MCA, revealed that while high PCs activity was detected in Control MDA-MB231 cells, the expression of ppFurin in these cells inhibited PCs enzymatic activity **(Figure 1a-1c)**. Similarly the expression of ppFurin in the melanoma cell line MDA-MB-435, also represses the PCs activity **(Figure 1b-1d)**. Using specific primers for the PCs found in the secretory pathway, namely Furin, PC5, PAEC4 and PC7 real-time PCR confirmed the presence of all these PCs in control MDA-MB-231 and MDA-MB-435 cells. In the presence of ppFurin, the mRNA level of Furin was reduced **(Figure 1e-1f)**.
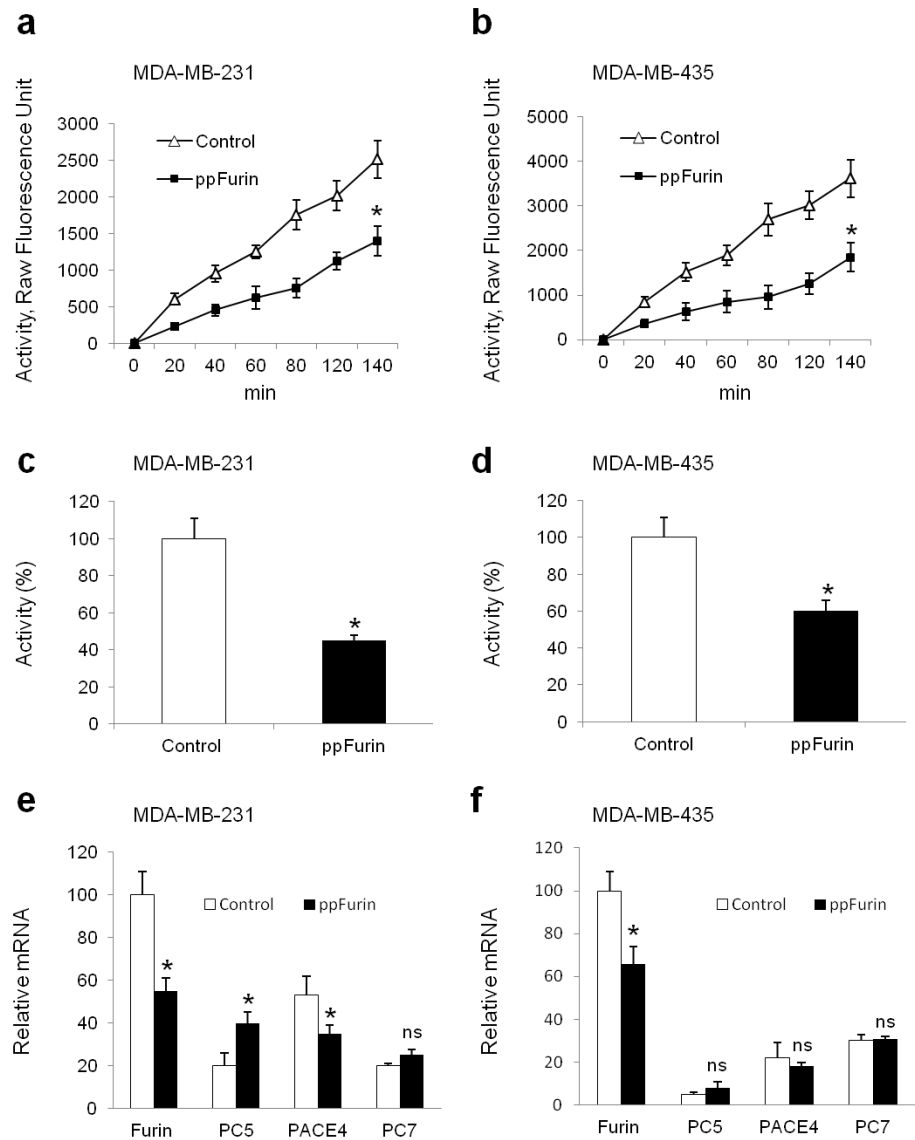
93

Figure 1. Inhibition of Furin activity by ppFurin in breast MDA-MB-231 and melanoma MDA-MB-435 cell lines. (**a, b**) MDA-MB-231 and MDA-MB-435 cells were stably transfected with pIRES2-EGFP empty vector (Control) or pIRES2-EGFP-ppFurin and the PCs activity was evaluated by the measurement of cell lysates ability to digest the universal PCs substrate pERTKR-MCA at the indicated time periods. (**c, d**) Bar graphs representing PCs activity of MDA-MB-231 and MDA-MB-435 cells at 2 hours of incubation in the absence and presence of ppFurin. (**e, f**) Real-time PCR analysis of indicted PCs expression in Control and ppFurin-expressing cells. Results are shown in the bar graphs and are expressed as the percentage of enzymatic activity or transcripts relative to controls (100%). All values are presented as means ± SEM of three independent experiments. Statistical significance was assessed by t-test and * represents $p < 0.05$ as compared to the corresponding controls.

To further confirm the effect of ppFurin on the enzymatic activity in MDA-MB-231 and MDA-MB-435 ppFurin expressing cells, we next assessed in these cells their ability to convert the human furin substrate proVEGF-C into the mature VEGF-C form. Immunoblotting analysis revealed that media derived from MDA-MB-231 and MDA-MB-435 cells transfected with a vector encoding proVEGF-C, mostly express the mature form of VEGF-C. Transfection of ppFurin expressing cells with vector encoding proVEGF-C showed reduction of the mature protein and enhanced the accumulation of the unprocessed form of VEGF-C (Figure 2a-2b). Similarly, immunoblotting analysis of the processing of the PCs substrate proIGF-1R revealed that MDA-MB-231 and MDA-MB-435 cell lines express proIGF-1R of which the processing of the β-subunit was also

113   blocked in MDA-MB-231 and MDA-MB-435 cells in the presence of ppFurin, as evidenced by the
114   accumulation of the precursor form and the reduction of the mature form of IGF-1R. For comparison
115   the processing of proVEGF-C and proIGF-1R was also examined in Control cells and in the presence
116   of the general PC-inhibitor α1-PDX. As illustrated, in α1-PDX-expressing cells, the accumulation of
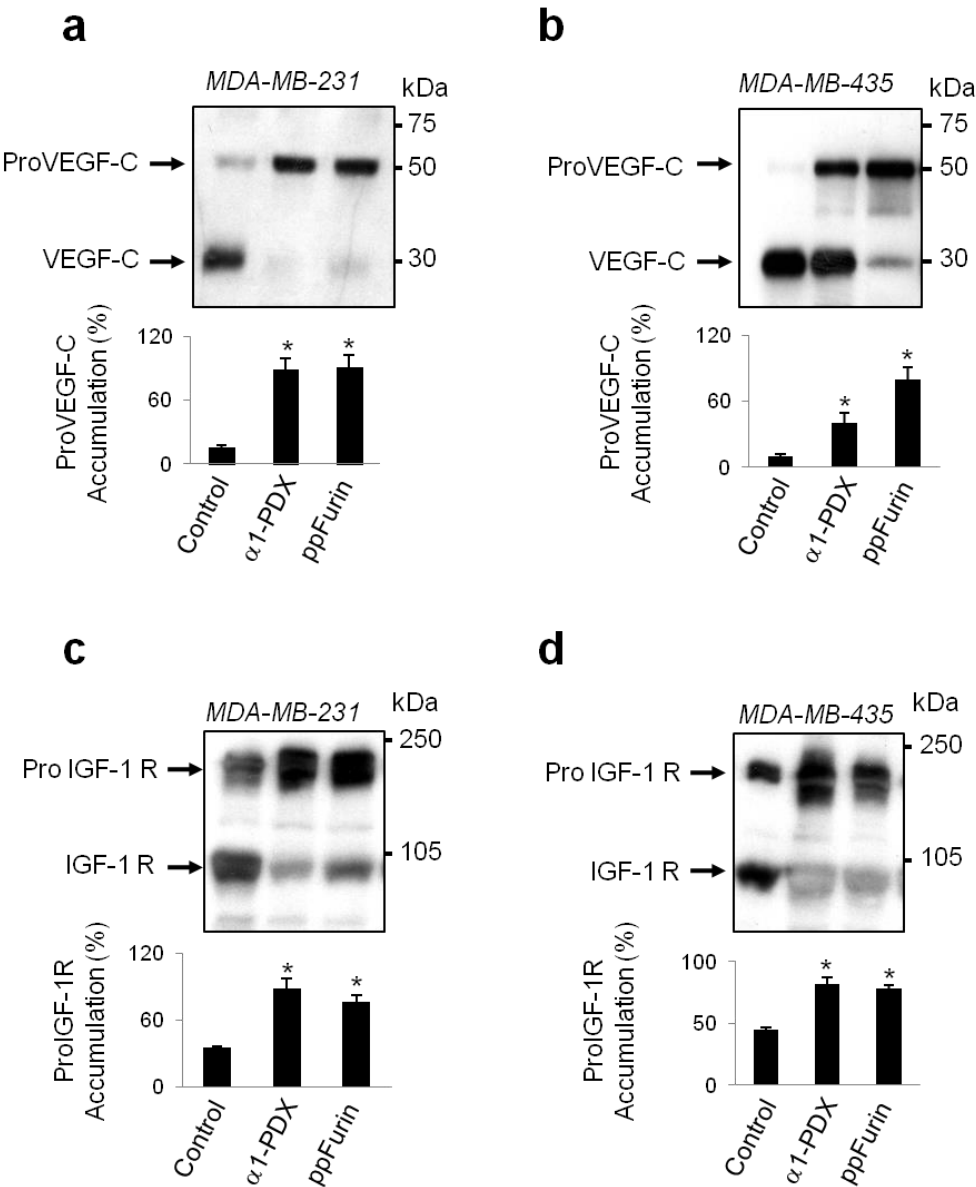117   proVEGF-C and proIGF-1R precursor forms was also enhanced (Figure 2).

118
119   **Figure 2.** Inhibition of proVEGF-C and proIGF-1R by ppFurin in breast MDA-MB-231 and melanoma
120   MDA-MB-435 cell lines. Western blotting for proVEGF-C precursor and its mature form (**a,b**) and for
121   proIGF-1R precursor and its mature form (**c,d**) expression. Effect of the general PC-inhibitor α1-PDX on
122   proVEGF-C and proGF-1R cleavage is given for comparison. Bar graphs indicate the percentages of
123   proVEGF-C and proIGF-1R accumulations in the absence and presence of ppFurin or α1-PDX. All values
124   are presented as means ± SEM of three independent experiments. Statistical significance was assessed by
125   t-test and * represents $p < 0.05$ as compared to the corresponding controls.

126   *2.2. Regulation of Ca²⁺ mobilization by ppFurin*

127   Next, we have investigated the possible effect of ppFurin on Ca^{2+} mobilization in MDA-MB-231
128   cells. As depicted in Figure 3a, in cells stably transfected with pIRES2-EGFP empty vector perfused
129   with a Ca^{2+}-free medium, treatment with the SERCA inhibitor TG led to a transient increase in $[Ca^{2+}]_i$

130   as a consequence of Ca^{2+} release from the intracellular stores. Subsequent re-addition of $CaCl_2$ to the
131   extracellular medium resulted in a further increase in $[Ca^{2+}]_i$ indicative of SOCE. Expression of
132   ppFurin significantly enhanced TG-evoked SOCE without having any effect on Ca^{2+} release from the
133   intracellular stores (Figure 3a). The effect of ppFurin was specific for MDA-MB-231 cells as it did not
134   have any effect on TG-induced Ca^{2+} mobilization in the melanoma cell line MDA-MB-435 (Figure
135   3b). Furthermore, we have found that expression of ppFurin in MDA-MB-231 cells leads to transient
136   constitutive Ca^{2+} entry detected as a rise in $[Ca^{2+}]_i$ upon re-addition of extracellular Ca^{2+} in the
137   absence of stimuli, while this effect was absent in MDA-MB-231 and MDA-MB-435 Control cells and
138   MDA-MB-435 stably expressing ppFurin (Figure 4a-d).
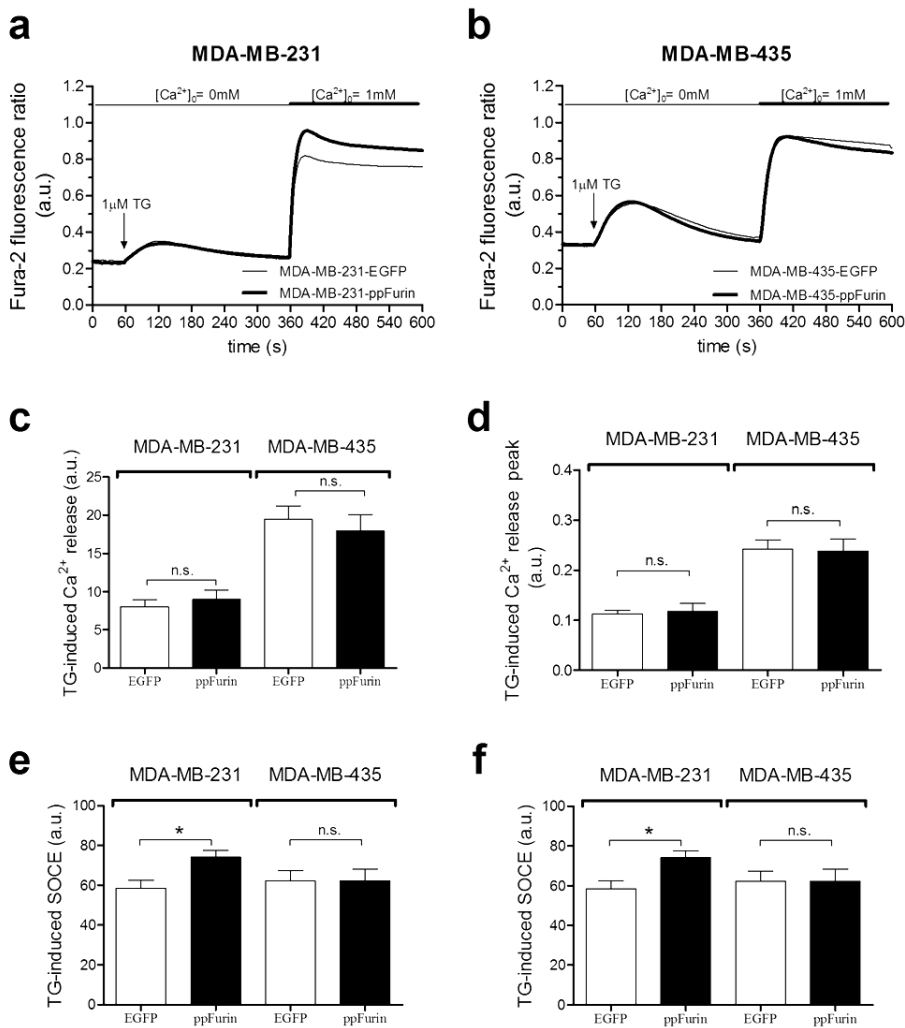

139

Figure 3. ppFurin enhances SOCE in MDA-MB-231 cells. Control MDA-MB-231 and MDA-MB-435 cells or
expressing ppFurin were loaded with fura-2- and perfused with a Ca^{2+} free medium (100 μM EGTA added) and
then stimulated with TG (1 μM) followed by reintroduction of external Ca^{2+} (final concentration 1 mM) to
initiate Ca^{2+} entry. (**a,b**) Traces are representative of 40 cells/day/3–5 days. (**c-f**) Bar graphs represent
TG-induced Ca^{2+} release and SOCE as the area under the curve (**c, e**) or the initial peak $[Ca^{2+}]_i$ elevation above
basal (**d, f**), expressed as mean ± SEM. Statistical significance was assessed by Student's t-test and * represents p
< 0.05 as compared to cells transfected with pIRES2-EGFP empty vector.

147

148   TRPC6 is upregulated in MDA-MB-231 cells and play a relevant role in the activation of SOCE
149   in these cells [18]. Hence, we have investigated whether TRPC6 mediates the increase in SOCE as
150   well as the constitutive Ca^{2+} entry observed in MDA-MB-231 cells in the presence of ppFurin. As

151   depicted in Figure 4e-h, TRPC6 expression silencing inhibits constitutive Ca^{2+} entry in
152   ppFurin-expressing cells, without having any effect in cells expression empty vector. As previously
153   reported [18], attenuation of TRPC6 expression in MDA-MB-231 cells transfected with pIRES2-EGFP
154   empty vector or ppFurin significantly inhibits SOCE with no change in Ca^{2+} release from the
155   intracellular stores (Figure 5c-h). Interestingly, in cells expressing ppFurin, TRPC6 expression
156   silencing resulted in a greater inhibition of SOCE than in mock-treated cells. As a result, SOCE in
157   ppFurin-expressing and control cells was comparable after TRPC6 knockdown (Figure 5f and 5h),
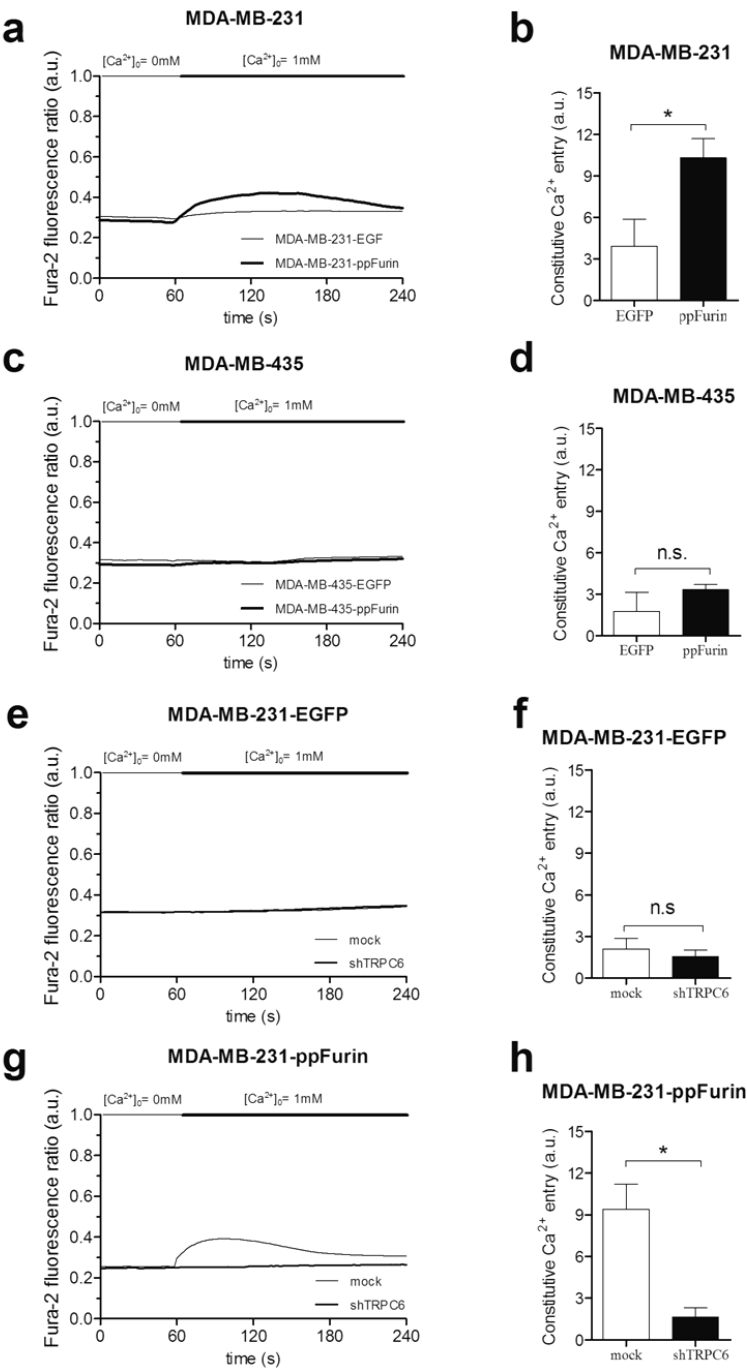158   thus indicating that TRPC6 is responsible for the increased SOCE in ppFurin-expressing cells.

159

160 **Figure 4.** ppFurin induces constitutive Ca^{2+} entry in MDA-MB-231 cells. (**a-d**) Control MDA-MB-231 and
161 MDA-MB-435 cells or expressing ppFurin were loaded with fura-2- and perfused with a Ca^{2+} free medium (100
162 μM EGTA added) and then were subjected to Ca^{2+} re-addition to determine the existence of constitutive Ca^{2+}
163 entry. (**e-h**) Control MDA-MB-231 and MDA-MB-435 cells or expressing ppFurin were transfected with
164 shTRPC6 or scramble plasmid, as indicated. Forty-eight hours after transfection, cells were with fura-2 and
165 perfused with a Ca^{2+}-free medium (100 μM EGTA added) and then were subjected to Ca^{2+} re-addition to
166 determine the existence of constitutive Ca^{2+} entry. Traces are representative of 40 cells/day/3–5 days. Bar graphs
167 represent constitutive Ca^{2+} entry as the area under the curve, expressed as mean ± SEM. Statistical significance
168 was assessed by Student's t-test and * represents $p < 0.05$ as compared to the corresponding control.
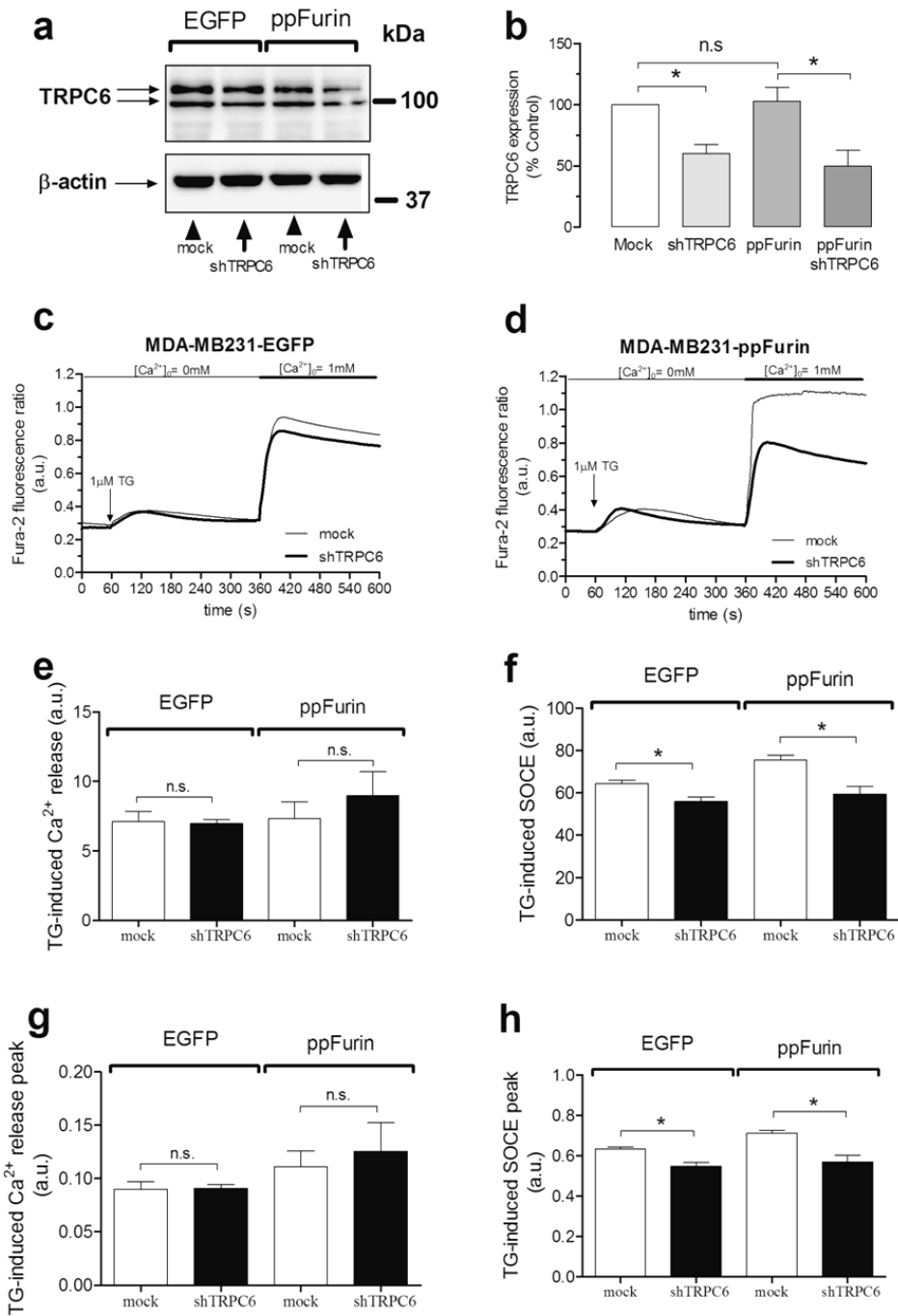

169

170 **Figure 5**. TRPC6 mediates the enhanced SOCE induced by ppFurin in MDA-MB-231 cells. (**a**) Control
171 MDA-MB-231 cells or the same cells expressing ppFurin were transfected with shTRPC6 or scramble plasmid,
172 as indicated. After 48 h cells were lysed and subjected to Western blotting using an anti-TRPC6 antibody,

173 followed by reprobing with anti-β-actin antibody for protein loading control. (**b**) Bar graphs represent TRPC6
174 expression under the different experimental conditions. (**c-h**) Control MDA-MB-231 cells or expressing ppFurin
175 were loaded with fura-2 and cells were perfused with a Ca^{2+}-free medium (100 μM EGTA added) and then
176 stimulated with TG (1 μM) followed by reintroduction of external Ca^{2+} (final concentration 1 mM) to initiate
177 Ca^{2+} entry. Traces are representative of 40 cells/day/3–5 days. (**e-h**) Bar graphs represent TG-induced Ca^{2+}
178 release and SOCE as the area under the curve (**e, g**) or the initial peak $[Ca^{2+}]_i$ elevation above basal (**f, h**),
179 expressed as mean ± SEM. Statistical significance was assessed by Student's t-test and * represents p < 0.05 as
180 compared to the respective control.

181 *2.3. Activation of TRPC6 Channels in MDA-MB-231 ppFurin-expressing cells*

182   Next, we explored the mechanism underlying the activation of TRPC6 by ppFurin. Our results
183 indicate that TRPC6 expression is similar in control and ppFurin-expressing cells (Figure 5a). TRPC6
184 has been reported to be activated by tyrosine phosphorylation [19], hence, we have explored
185 whether ppFurin is able to induce TRPC6 tyrosine phosphorylation in MDA-MB-231 cells. As
186 depicted in Figure 6, in MDA-MB-231 cells transfected with pIRES2-EGFP empty vector treatment
187 with TG resulted in a significant increase in the phosphotyrosine level of TRPC6. Interestingly,
188 expression of ppFurin in these cells significantly increased TRPC6 tyrosine phosphorylation, and
189 thus activation, under resting conditions and TG was unable to induce further increase in the
190 phosphotyrosine level of the channel (Figure 6). These findings might explain the constitutive Ca^{2+}
191 entry as well as the increase in SOCE induced by ppFurin in MDA-MB-231 cells.
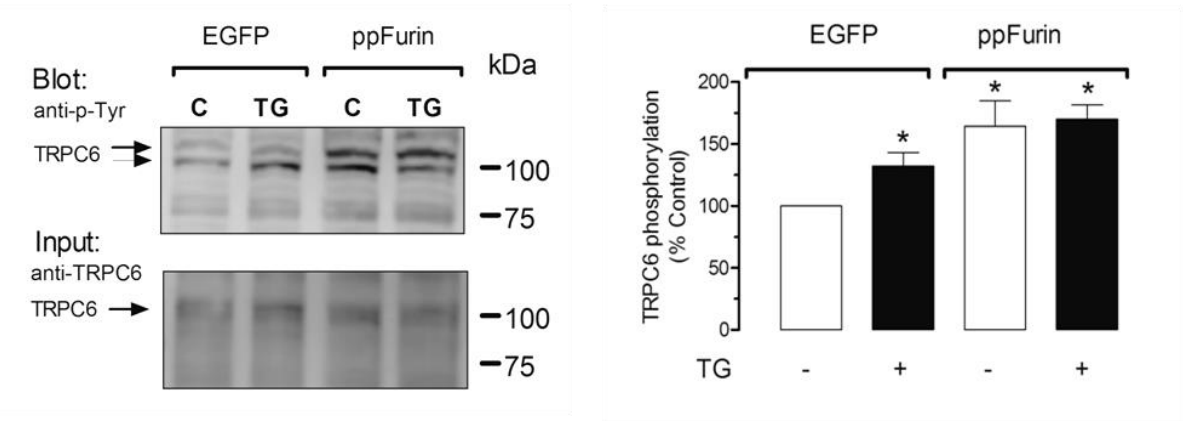
192

193

194 **Figure 6.** ppFurin induces TRPC6 tyrosine phosphorylation in MDA-MB-231 cells. Control MDA-MB-231 cells
195 or expressing ppFurin were stimulated with 1 μM TG for 3 min or left untreated and lysed. Whole cell lysates
196 were immunoprecipitated (IP) with anti-TRPC6 antibody and immunoprecipitates were subjected to 10%
197 SDS-PAGE and subsequent Western blotting with specific anti-phosphotyrosine antibody, as indicated.
198 Membranes were reprobed with the antibody used for immunoprecipitation for protein loading control. The
199 panels show results from one experiment representative of five others. Bar graphs represent the quantification
200 of TRPC6 tyrosine phosphorylation in resting and TG-treated cells. Results are presented as percentage of
201 control (cells transfected with pIRES2-EGFP empty vector and not stimulated with TG) and expressed as mean
202 ± S.E.M. Statistical significance was assessed by one-way analysis of variance combined with the Dunnett post
203 hoc test and * represents p < 0.05 as compared to control.

204 *2.3. Inhibition of MDA-MB-231 malignant phenotype by ppFurin*

205   Previously induction of TRPC6 was reported to promote the aggressive phenotype of various
206 cancer cells by promoting a sustained elevation of intracellular Ca^{2+} level, which is critical for cancer
207 cells proliferation and migration **[18]**. While other studies reported that TRPC6 overactivation

208   mediated a significant reduction in breast cancer cells growth and viability **[20]**. Thereby, we first
209   determined whether the TRPC6 activation in ppFurin-expressing MDA-MB-231 cells was
210   accompanied by alteration in their viability and resistance to the apoptotic agent hydrogen peroxide
211   (H_2O_2). Thereby, cells were treated for 6 h with various concentration of H_2O_2 and the cytotoxic effect
212   was evaluated using the MTT assay (Figure 7a). As illustrated, H_2O_2 inhibited MDA-MB-231 cells
213   viability in a dose-dependent manner that was further enhanced in the presence of ppFurin (Figure
214   7a). Similarly using cell motility and collagen invasion assays revealed that the expression of
215   ppFurin in these cells delayed MDA-MB-231 monolayer repair following a scratch wound (Figure
216   7b-c) and repressed their ability to invade collagen (Figure 7d-e), respectively.
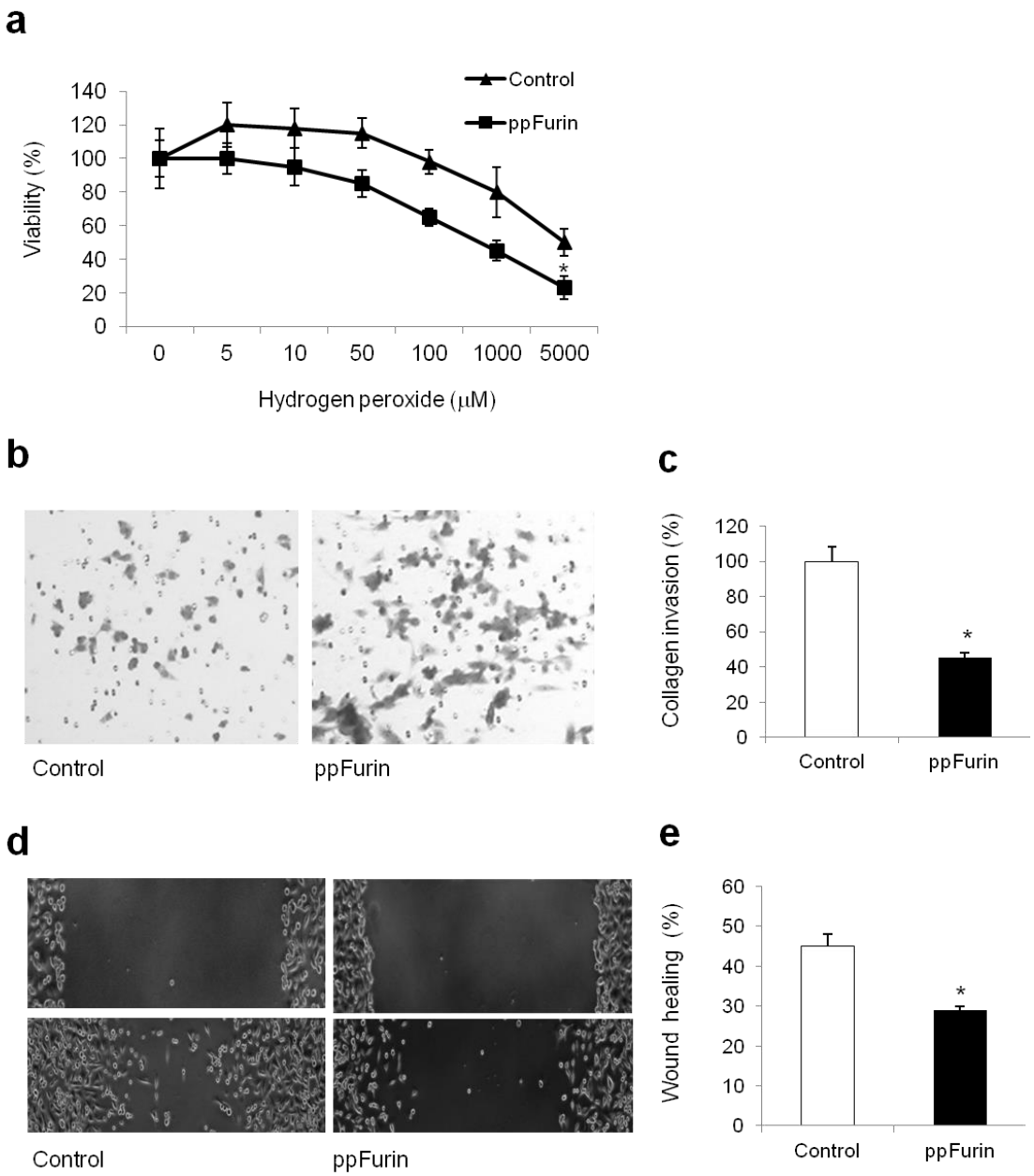
Figure 7. ppFurin enhances MDA-MB-231 cells sensitization to hydrogen peroxide (H_2O_2) and reduces cell
invasion and motility. (**a**) Effect of hydrogen peroxide on Control and ppFurin-expressing MDA-MB-231 cells
viability as assessed by MTT assay and calculated with respect to control, which is set as 100%. (**b**) Control and
ppFurin-expressing MDA-MB-231 cells were incubated in a microchemotaxis chamber pre-coated with collagen

222 IV for cell invasion assay, as indicated. (**c**) The results are represented as the percentage of invading cells. (**d**)
223 Cell motility was analyzed by scratch wound assay. Control and ppFurin-expressing MDA-MB-231 cells were
224 subjected to scratch wounds and imaged after 24 hours (n = 6/well). (**e**) Quantification of wound closure after 24
225 hours of Control MDA-MB-231 cells and the same cells stably expressing ppFurin. All data are representative of
226 3 experiments and shown as mean ± S.E.M (n=3 per group). *P < 0.05. Student's t test was applied for statistical
227 analysis. P values of <0.05 were considered significant.

3. Discussion

229   Proteolytic maturation of protein precursors by furin is involved in various cellular
230 mechanisms directly responsible for the malignant phenotype of a variety of tumors including
231 breast cancers [21–23]. These processes often involve the activation of proteins required for cell
232 proliferation, invasion and signaling pathways that sustain cancer cell growth and viability [21–23].
233 We have previously reported that inhibition of protein precursors cleavage can affect these processes
234 in different tumor cell types [9–12,14]. In particular, inhibition of the proprotein convertases (PCs) by
235 the exogenous general PCs inhibitor α1-PDX elicits the repression of the activity of all the PCs found
236 in the secretory pathway leading to the inhibition of a variety of growth factors, receptors and
237 proteases resulting in reduced tumor cells proliferation, invasion and/or survival [9–12,14].

238   Since Ca^{2+} signaling and various Ca^{2+} regulating proteins known to be involved in breast tumor
239 development and progression are substrates and/or downsteam effectors of the ubiquitously
240 expressed PC furin [10,25], we thought that ppFurin [24], its naturally occurring inhibitor, might be
241 involved in the regulation of Ca^{2+} mobilization in breast cancer cells. By analyzing the effect of stable
242 expression of ppFurin on PCs activity in MDA-MB-231 breast cancer and MDA-MB-435 melanoma
243 cells, we found that ppFurin reduces significantly the *in vitro* enzymatic activity of PCs. This was
244 confirmed following the analysis of two distinct furin substrates: proVEGF-C and proIGF-1R and
245 found that ppFurin was driving in the two cell lines the cleavage repression of these protein
246 precursors. Further analysis revealed that expression of ppFurin in MDA-MB-231 but not in
247 MDA-MB-435 melanoma cells significantly induces constitutive Ca^{2+} entry. This Ca^{2+} mobilization
248 was found to imply TRPC6 activation, since constitutive Ca^{2+} entry was disturbed following
249 silencing of TRPC6 expression, as assessed by means of shRNA gene knockdown approach.

250   Targeting altered Ca^{2+} homeostasis in cancer cells was previously proposed as a potential
251 anti-cancer strategy. This by interfering with the expression and/or the activity of Ca^{2+}-handling
252 proteins. Indeed, the activity of various Ca^{2+} channels is known to be important in the control of
253 cancer cells growth and survival [4,25]. Specifically, TRPC6 channels are well established to be
254 implicated in cell proliferation and migration [26] and various hypertrophic gene expression and
255 reported to be mediated by NFAT pathway activation in normal [27] and cancer [28] cells. In this
256 aspect, inhibition of TRPC6 expression or activity was suggested to be applied to target breast cancer
257 cell proliferation and migration [26]. In the current studies, we found that TRPC6 phosphorylation
258 was up-regulated in MDA-MB-231 ppFurin-expressing cells while compared to control
259 MDA-MB-231 cells, leading to an increased SOCE and was associated with reduced cell growth and
260 survival. The relevance of TRPC6 hyperactivity in the inhibition of cell growth and induction of
261 apoptosis has been previously demonstrated [29]. Indeed, while TRPC6 activation is known to
262 promote cell proliferation, its overactivation by hyperforin was reported to induce a significant
263 disorder in Ca^{2+} signaling that affect cell proliferation and induces apoptosis in cancer cells [20,30].
264 Similarly, extended enhance in $[Ca^{2+}]_i$ was reported to activate various apoptotic cascades that
265 encouraged the use of drugs able to maintain enhanced $[Ca^{2+}]_i$ in cancer treatment. These include

266 topotecan [31], arsenic trioxide (As$_2$O$_3$) [32] and 5-Fluorouracil (5-FU) [33] all induce intracellular
267 Ca^{2+} alteration that leads to apoptosis. For example 5-FU that is used for the treatment of various
268 cancers, including breast cancer, involved the elevation of [Ca^{2+}]$_i$ that activates p53 resulting in the
269 activation of caspases and lately apoptosis [33,34]. In addition to cell growth and proliferation, Ca^{2+}
270 signaling also plays a central regulatory role in migration [35]. We found that TRPC6
271 hyperactivation in response to ppFurin expression also inhibited MDA-MB-231 cell migration and
272 invasion. Although how TRPC6 hyperactivation affect MDA-MB 231 cells motility, is quite unclear,
273 the role of TRPC6 in the regulation of actin cytoskeleton system activity may be the major
274 contributing factor. Indeed, TRPC6-mediated Ca^{2+} influx was reported to be directly associated with
275 actin cytoskeleton that is responsible for the regulation of cell morphology, cell adhesion, and
276 motility [35]. While the TRPC6-mediated Ca^{2+} entry was found to contribute to migration and
277 invasion, the gain-of-function mutation of TRPC6 found in several podocytes leads to focal and
278 segmental glomerulosclerosis (FSGS), a leading cause of glomerulonephritis and chronic kidney
279 disease [36,37] and proteinuria [38] due to alteration of actin organization and subsequently cell
280 migration repression. In addition, exaggerated Ca^{2+} signaling mediated by these TRPC6 mutations
281 was also found to cause apoptosis [37].

282   An increasing number of studies have identified a wide range of protein precursors in breast
283 cancer cells of which the cleavage and activity are inhibited by furin repression [21,23,24,39,40].
284 These studies highlight the important role for the cleavage of these protein precurssors in breast
285 cancer development and progression and reveals that their cleavage inhbition results in tumor cells
286 proliferation, invasion and survival inhibition. However, further investigations are needed to
287 explore the effect of specific protein precursor cleavage inhibition on TRPC6-mediated Ca2+ entry.

288 **4. Materials and Methods**

289 4.1. Materials and reagents

290   Fura-2 acetoxymethyl ester (fura-2/AM) was from Molecular Probes (Leiden, The Netherlands).
291 Thapsigargin (TG) was from Sigma-Aldrich (Madrid, Spain). Rabbit polyclonal anti-TRPC6 antibody
292 (catalog number: TA328771, corresponding to amino acid residues 573-586 of rat TRPC6, 2nd
293 extracellular loop) was from Origene (Rockville, MD, USA). The anti–Insulin-like growth factor I
294 receptor (IGF-1R) and anti-Vascular endothelial growth factor C (VEGF-C) were from Santa Cruz.
295 Mouse-monoclonal anti-phosphotyrosine antibody (catalog number: 05-321) was from Millipore
296 (Temecula, CA, USA). All other reagents were of analytical grade.

297 4.2. Cell culture and Transfections.

298   The human breast cancer MDA-MB-231 and the melanoma MDA-MB 435 cell lines were stably
299 transfected with pIRES2–enhanced green fluorescent protein (EGFP) empty vector or the same
300 vector expressing the ppFurin cDNA. In other experiments, cancer MDA-MB-231 and the melanoma
301 MDA-MB 435 cell lines were transiently transfected with pcDNA3-zeo-Flag.cm5 empty vector or the
302 same vector containing wild-type VEGF-C. Transfections were carried out using the Effectene
303 transfection reagent (Qiagen) according to manufacturer's instructions and stably
304 ppFurin-expressing cells were selected using G418 resistance, as previously described **[41,42]**. Cells
305 were grown in DMEM supplemented with 10% FCS, 100 units/ml penicillin, and 100 mg/ml
306 streptomycin.

307 4.3. RNA extraction and real time PCR

308   Total RNA extraction was performed using the Macherey-Nagel RNA isolation kit that includs
309 DNase treatment (Qiagen), according to the manufacturer's instructions. The RNA was reverse
310 transcribed using the high capacity cDNA reverse transcription kit (Applied Biosystems,
311 Courtaboeuf, France) and used for real time PCR in the presence of specific primers and Power
312 SYBR Green PCR Master Mix (Applied Biosystems), as previously described [7,9]. The qPCR data
313 were acquired with the StepOnePlusTM Real-Time PCR System (Applied Biosystems, Courtaboeuf,
314 France). The expression levels were normalized to human GAPDH.

315 4.4. Immunoprecipitation and Western blotting

316   Immunoprecipitation and Western blotting were performed as described previously **[43]**.
317 Briefly, 500 µL aliquots of cell suspension (18 × 106 cell/mL) were lysed with an equal volume of
318 ice-cold 2 × NP-40 buffer, containing 274 mM NaCl, 40 mM Tris, 4 mM EDTA, 20% glycerol, 2%
319 nonidet P-40, 2 mM Na_3VO_4 and complete EDTA-free protease inhibitor tablets. Samples of cell
320 lysates (1 mL) were immunoprecipitated by incubation with 2.5 µg of anti-TRPC6 and 50 µL of
321 protein A-agarose overnight at 4 °C on a rotary platform. The immunoprecipitates were resolved by
322 10% SDS-PAGE and separated proteins were electrophoreticcally transferred onto nitrocellulose
323 membranes for subsequent probing. Blots were incubated for 3 h at room temperature with 10%
324 (w/v) BSA in tris-buffered saline with 0.1% Tween 20 (TBST) to block residual protein binding sites.
325 Immunodetection of phosphotyrosine and TRPC6 were achieved by incubation overnight with
326 anti-phosphotyrosine antibody diluted 1:500 in TBST and overnight with anti-TRPC6 antibody
327 diluted in 1:500 in TBST. The primary antibody was removed and blots were washed three times for
328 10 min each with TBST. Following, Primary antibodies were detected by incubation for 1 h with
329 horseradish peroxidase-conjugated goat anti-mouse IgG antibody or horseradish
330 peroxidase-conjugated goat anti-rabbit IgG antibody diluted 1:10000 in TBST and then exposed to
331 enhanced chemiluminiscence reagents for 5 min. IGF-1R and VEGF-C cleavage detection by Western
332 blotting analysis was performed as previously described [9,17]. The density of bands was measured
333 using C-DiGit Chemiluminescent Western Blot Scanner and ImageJ software (NIH, U.S.A.). Data
334 were normalized to the amount of protein recovered by the antibody used for the
335 immunoprecipitation.

336 4.5. Determination of cytosolic free-Ca^{2+} concentration

337   Cells were loaded with fura-2 by incubation with 2 µM fura 2/AM for 30 min at 37 °C.
338 Coverslips with cultured cells were mounted on a perfusion chamber and placed on the stage of an
339 epifluorescence inverted microscope (Nikon Eclipse Ti2, Amsterdam, The Netherlands) with image
340 acquisition and analysis software for videomicroscopy (NIS-Elements Imaging Software, Nikon).
341 Cells were superfused with HEPES-buffered saline (HBS) containing (in mM): 125 NaCl, 5 KCl, 1
342 MgCl2, 5 glucose, 25 HEPES, and pH 7.4, supplemented with 0.1% (w/v) BSA, and were
343 alternatively excited with light from a xenon lamp passed through a high-speed monochromator
344 (Optoscan ELE 450, Cairn Research, Faversham, UK) at 340/380 nm. Fluorescence emission at 505 nm
345 was detected using a sCMOS camera (Zyla 4.2, Andor, Belfast, UK) and recorded using
346 NIS-Elements AR software (Nikon, Amsterdam, The Netherlands). Fluorescence ratio (F340/F380)
347 was calculated pixel by pixel **[44]**. TG-evoked Ca2+ release and SOCE were measured as the integral
348 of the rise in the fura-2 fluorescence ratio for 2½ min after the addition of TG or Ca^{2+}, respectively.

349 4.6. Cell Viability Assay

350   The cell viability was evaluated using the MTT assay, as previously described **[45]**. Control and
351 MDA-MB-231 ppFurin cells were plated in 96-well microtiter plates respectively at a density of (1 ×
352 10^4/ml) cells/well. Next day, the cells were treated with various concentration of H_2O_2 for 6h and
353 were immersed with MTT solution (0.5 mg/mL) for 3 h at 37 °C. Then absorbance was measured at
354 570 nm using ELISA plate reader. The viability was calculated with respect to control, which is set as
355 100%.

356   4.7. Cell invasion assay

357   The *in vitro* invasion activity of control and MDA-MB-231 ppFurin-expressing cells was
358   performed using 24-well microchemotaxis chambers precoated with 7.5 μg collagen type IV (Becton
359   Dickinson Labware), as previously described [17,21]. Tumor cells (1×10^5/ml) were resuspended in
360   serum-free media and were loaded into the upper chamber of Transwells. Cells were incubated at
361   37°C for 24 h and invasion across collagen layer was initiated by adding 10% FBS (chemoattractant)
362   to the lower chamber. Cells detected in each well were counted and the results were represented as
363   (number of migrated cells/number of total cells) × 100%.

364   4.8. Wound-healing assay

365   The wound-healing assay was conducted as previously reported [39]. Briefly, control and
366   MDA-MB-231 ppFurin-expressing cells were seeded into 6-well plate at 5×10^5/well and grown in
367   growth media until 90–100% confluency. A cell-free area (wound) within the cell monolayer was
368   constructed using a sterile micropipette tip. Healing of the wound was observed after 24 h by a light
369   microscopy and analyzed using Image J software. The area that remained clear of cells after this
370   period was quantified and compared with the area of the wound at time 0.

371   4.9. Statistical analysis

372   All data are presented as ± standard error of mean (SEM) unless specifically mentioned.
373   Student's t test or one-way analysis of variance combined with the Dunnett post hoc test were
374   applied for statistical analysis, as appropriate. P values of <0.05 were considered significant.

375   **5. Conclusions**

376   Our work shows that expression of ppFurin, a naturally occurring inhibitor of the convertase
377   Furin mediates an activation of TRPC6 that induces enhanced Ca^{2+} influx in breast cancer cells,
378   driving their reduced viability and migration and their enhanced sensitization to the apoptotic agent
379   hydrogen peroxide. Thus, interfering with furin activity-mediated Ca^{2+} mobilization and TRPC6
380   activation represent a potential strategy controlling malignant phenotype and resistance to therapy
381   in breast cancer cells. Prospect studies based on our conclusion will validate the efficacy of
382   overactivation of TRPC6 in breast cancer repression using *in vivo* models.
383

384   **Author Contributions:**

385   Conceptualization, J.A.R., G.S., S.E., and AM. K.; methodology, J.J.L.,G.S., C.C., S.P., J.D., I.B., and
386   T.S.; investigation, J.A.R., and AM.K.; Funding acquisition, J.A.R., G.S., S.E., and AM. K.;
387   writing—original draft preparation,—review and editing, J.A.R., G.S., S.E., and AM.K.; project
388   administration, J.A.R., and AM.K. All authors have read and agreed to the published version of the
389   manuscript.
390

398   **Conflicts of Interest:**
399   The authors declare no conflict of interest.
400

401   **References**

402   1.   Momenimovahed, Z.; Salehiniya, H. Epidemiological characteristics of and risk factors for breast cancer in
403   the world. *Breast Cancer (Dove Med Press)* **2019**, *11*, 151–164, doi:10.2147/BCTT.S176070.
404   2.   Prevarskaya, N.; Ouadid-Ahidouch, H.; Skryma, R.; Shuba, Y. Remodelling of Ca2+ transport in cancer:
405   how it contributes to cancer hallmarks? *Philos Trans R Soc Lond B Biol Sci* **2014**, *369*,
406   doi:10.1098/rstb.2013.0097.
407   3.   Azimi, I.; Roberts-Thomson, S.J.; Monteith, G.R. Calcium influx pathways in breast cancer: opportunities
408   for pharmacological intervention. *Br J Pharmacol* **2014**, *171*, 945–960, doi:10.1111/bph.12486.
409   4.   Stewart, T.A.; Yapa, K.T.D.S.; Monteith, G.R. Altered calcium signaling in cancer cells. *Biochimica et
410   Biophysica Acta (BBA) - Biomembranes* **2015**, *1848*, 2502–2511, doi:10.1016/j.bbamem.2014.08.016.
411   5.   Siegfried, G.; Descarpentrie, J.; Evrard, S.; Khatib, A.-M. Proprotein convertases: Key players in
412   inflammation-related   malignancies   and   metastasis.   *Cancer   Lett.*   **2020**,   *473*,   50–61,
413   doi:10.1016/j.canlet.2019.12.027.
414   6.   Sfaxi, F.; Scamuffa, N.; Lalou, C.; Ma, J.; Metrakos, P.; Siegfried, G.; Ragg, H.; Bikfalvi, A.; Calvo, F.; Khatib,
415   A.-M. Repression of liver colorectal metastasis by the serpin Spn4A a naturally occurring inhibitor of the
416   constitutive secretory proprotein convertases. *Oncotarget* **2014**, *5*, 4195–4210, doi:10.18632/oncotarget.1966.
417   7.   Scamuffa, N.; Basak, A.; Lalou, C.; Wargnier, A.; Marcinkiewicz, J.; Siegfried, G.; Chrétien, M.; Calvo, F.;
418   Seidah, N.G.; Khatib, A.-M. Regulation of prohepcidin processing and activity by the subtilisin-like
419   proprotein convertases Furin, PC5, PACE4 and PC7. *Gut* **2008**, *57*, 1573–1582, doi:10.1136/gut.2007.141812.
420   8.   Adam*, F.; Khatib*, A.-M.; Lopez, J.J.; Vatier, C.; Turpin, S.; Muscat, A.; Soulet, F.; Aries, A.; Jardin, I.; Bobe,
421   R.; et al. Apelin: an antithrombotic factor that inhibits platelet function. *Blood* **2016**, *127*, 908–920,
422   doi:10.1182/blood-2014-05-578781 * equal contribution.
423   9.   Scamuffa, N.; Sfaxi, F.; Ma, J.; Lalou, C.; Seidah, N.; Calvo, F.; Khatib, A.-M. Prodomain of the proprotein
424   convertase subtilisin/kexin Furin (ppFurin) protects from tumor progression and metastasis. *Carcinogenesis*
425   **2014**, *35*, 528–536, doi:10.1093/carcin/bgt345.
426   10. Lahlil, R.; Calvo, F.; Khatib, A.-M. The potential anti-tumorigenic and anti-metastatic side of the proprotein
427   convertases inhibitors. *Recent Pat Anticancer Drug Discov* **2009**, *4*, 83–91, doi:10.2174/157489209787002470.
428   11. Basak, A.; Khatib, A.-M.; Mohottalage, D.; Basak, S.; Kolajova, M.; Bag, S.S.; Basak, A. A novel enediynyl
429   peptide inhibitor of furin that blocks processing of proPDGF-A, B and proVEGF-C. *PLoS ONE* **2009**, *4*,
430   e7700, doi:10.1371/journal.pone.0007700.
431   12. He, Z.; Thorrez, L.; Siegfried, G.; Meulemans, S.; Evrard, S.; Tejpar, S.; Khatib*, A.-M.; Creemers*, J.W.M.
432   The proprotein convertase furin is a pro-oncogenic driver in KRAS and BRAF driven colorectal cancer.
433   *Oncogene* **2020**, *39*, 3571-3587. *Equal contribution, doi:10.1038/s41388-020-1238-z.
434   13. Creemers, J.W.M.; Khatib, A.-M. Knock-out mouse models of proprotein convertases: unique functions or
435   redundancy? *Front. Biosci.* **2008**, *13*, 4960–4971, doi:10.2741/3055.
436   14. Tomé, M.; Pappalardo, A.; Soulet, F.; López, J.J.; Olaizola, J.; Leger, Y.; Dubreuil, M.; Mouchard, A.; Fessart,
437   D.; Delom, F.; et al. Inactivation of Proprotein Convertases in T Cells Inhibits PD-1 Expression and Creates
438   a Favorable Immune Microenvironment in Colorectal Cancer. *Cancer Res.* **2019**, *79*, 5008–5021,
439   doi:10.1158/0008-5472.CAN-19-0086.
440   15. Khatib, A.-M.; Siegfried, G.; Chrétien, M.; Metrakos, P.; Seidah, N.G. Proprotein Convertases in Tumor
441   Progression and Malignancy. *Am J Pathol* **2002**, *160*, 1921–1935.
442   16. Ma, J.; Evrard, S.; Badiola, I.; Siegfried, G.; Khatib, A.-M. Regulation of the proprotein convertases
443   expression and activity during regenerative angiogenesis: Role of hypoxia-inducible factor (HIF). *Eur. J.
444   Cell Biol.* **2017**, *96*, 457–468, doi:10.1016/j.ejcb.2017.06.001.

17. Lalou, C.; Scamuffa, N.; Mourah, S.; Plassa, F.; Podgorniak, M.-P.; Soufir, N.; Dumaz, N.; Calvo, F.; Basset-Seguin, N.; Khatib, A.-M. Inhibition of the proprotein convertases represses the invasiveness of human primary melanoma cells with altered p53, CDKN2A and N-Ras genes. *PLoS ONE* **2010**, *5*, e9992, doi:10.1371/journal.pone.0009992.

18. Jardin, I.; Diez-Bello, R.; Lopez, J.J.; Redondo, P.C.; Salido, G.M.; Smani, T.; Rosado, J.A. TRPC6 Channels Are Required for Proliferation, Migration and Invasion of Breast Cancer Cell Lines by Modulation of Orai1 and Orai3 Surface Exposure. *Cancers (Basel)* **2018**, *10*, doi:10.3390/cancers10090331.

19. Hisatsune, C.; Kuroda, Y.; Nakamura, K.; Inoue, T.; Nakamura, T.; Michikawa, T.; Mizutani, A.; Mikoshiba, K. Regulation of TRPC6 channel activity by tyrosine phosphorylation. *J. Biol. Chem.* **2004**, *279*, 18887–18894, doi:10.1074/jbc.M311274200.

20. Aydar, E.; Yeo, S.; Djamgoz, M.; Palmer, C. Abnormal expression, localization and interaction of canonical transient receptor potential ion channels in human breast cancer cell lines and tissues: a potential target for breast cancer diagnosis and therapy. *Cancer Cell Int* **2009**, *9*, 23, doi:10.1186/1475-2867-9-23.

21. He, Z.; Khatib, A.-M.; Creemers, J.W.M. Loss of the proprotein convertase Furin in T cells represses mammary tumorigenesis in oncogene-driven triple negative breast cancer. *Cancer Lett.* **2020**, *484*, 40–49, doi:10.1016/j.canlet.2020.05.001.

22. Khatib, A.-M.; Siegfried, G.; Chrétien, M.; Metrakos, P.; Seidah, N.G. Proprotein convertases in tumor progression and malignancy: novel targets in cancer therapy. *Am. J. Pathol.* **2002**, *160*, 1921–1935, doi:10.1016/S0002-9440(10)61140-6.

23. Siegfried, G.; Descarpentrie, J.; Evrard, S.; Khatib, A.-M. Proprotein convertases: Key players in inflammation-related malignancies and metastasis. *Cancer Lett.* **2020**, *473*, 50–61, doi:10.1016/j.canlet.2019.12.027.

24. Thomas, G. Furin at the cutting edge: from protein traffic to embryogenesis and disease. *Nat. Rev. Mol. Cell Biol.* **2002**, *3*, 753–766, doi:10.1038/nrm934.

25. Leverrier-Penna, S.; Destaing, O.; Penna, A. Insights and perspectives on calcium channel functions in the cockpit of cancerous space invaders. *Cell Calcium* **2020**, *90*, 102251, doi:10.1016/j.ceca.2020.102251.

26. Jardin, I.; Diez-Bello, R.; Lopez, J.J.; Redondo, P.C.; Salido, G.M.; Smani, T.; Rosado, J.A. TRPC6 Channels Are Required for Proliferation, Migration and Invasion of Breast Cancer Cell Lines by Modulation of Orai1 and Orai3 Surface Exposure. *Cancers (Basel)* **2018**, *10*, doi:10.3390/cancers10090331.

27. Kuwahara, K.; Wang, Y.; McAnally, J.; Richardson, J.A.; Bassel-Duby, R.; Hill, J.A.; Olson, E.N. TRPC6 fulfills a calcineurin signaling circuit during pathologic cardiac remodeling. *J. Clin. Invest.* **2006**, *116*, 3114–3126, doi:10.1172/JCI27702.

28. Kim, J.-H.; Hwang, K.-H.; Eom, M.; Kim, M.; Park, E.Y.; Jeong, Y.; Park, K.-S.; Cha, S.-K. WNK1 promotes renal tumor progression by activating TRPC6-NFAT pathway. *FASEB J.* **2019**, *33*, 8588–8599, doi:10.1096/fj.201802019RR.

29. Aydar, E.; Yeo, S.; Djamgoz, M.; Palmer, C. Abnormal expression, localization and interaction of canonical transient receptor potential ion channels in human breast cancer cell lines and tissues: a potential target for breast cancer diagnosis and therapy. *Cancer Cell International* **2009**, *9*, 23, doi:10.1186/1475-2867-9-23.

30. Donà, M.; Dell'Aica, I.; Pezzato, E.; Sartor, L.; Calabrese, F.; Della Barbera, M.; Donella-Deana, A.; Appendino, G.; Borsarini, A.; Caniato, R.; et al. Hyperforin inhibits cancer invasion and metastasis. *Cancer Res.* **2004**, *64*, 6225–6232, doi:10.1158/0008-5472.CAN-04-0280.

486   31.   Oberhoff, C.; Kieback, D.G.; Würstlein, R.; Deertz, H.; Sehouli, J.; van Soest, C.; Hilfrich, J.; Mesrogli, M.;
487   von Minckwitz, G.; Staab, H.J.; et al. Topotecan chemotherapy in patients with breast cancer and brain
488   metastases: results of a pilot study. *Onkologie* **2001**, *24*, 256–260, doi:10.1159/000055088.

489   32.   Ahn, R.W.; Chen, F.; Chen, H.; Stern, S.T.; Clogston, J.D.; Patri, A.K.; Raja, M.R.; Swindell, E.P.; Parimi, V.;
490   Cryns, V.L.; et al. A Novel Nanoparticulate Formulation of Arsenic Trioxide with Enhanced Therapeutic
491   Efficacy in a Murine Model of Breast Cancer. *Clin Cancer Res* **2010**, *16*, 3607–3617,
492   doi:10.1158/1078-0432.CCR-10-0068.

493   33.   Longley, D.B.; Harkin, D.P.; Johnston, P.G. 5-fluorouracil: mechanisms of action and clinical strategies. *Nat.*
494   *Rev. Cancer* **2003**, *3*, 330–338, doi:10.1038/nrc1074.

495   34.   Petak, I.; Tillman, D.M.; Houghton, J.A. p53 Dependence of Fas Induction and Acute Apoptosis in
496   Response to 5-Fluorouracil-Leucovorin in Human Colon Carcinoma Cell Lines. *Clin Cancer Res* **2000**, *6*,
497   4432–4441.

498   35.   Singh, I.; Knezevic, N.; Ahmmed, G.U.; Kini, V.; Malik, A.B.; Mehta, D. Gαq-TRPC6-mediated Ca2+ Entry
499   Induces RhoA Activation and Resultant Endothelial Cell Shape Change in Response to Thrombin. *J. Biol.*
500   *Chem.* **2007**, *282*, 7833–7843, doi:10.1074/jbc.M608288200.

501   36.   Winn, M.P.; Conlon, P.J.; Lynn, K.L.; Farrington, M.K.; Creazzo, T.; Hawkins, A.F.; Daskalakis, N.; Kwan,
502   S.Y.; Ebersviller, S.; Burchette, J.L.; et al. A Mutation in the TRPC6 Cation Channel Causes Familial Focal
503   Segmental Glomerulosclerosis. *Science* **2005**, *308*, 1801–1804, doi:10.1126/science.1106215.

504   37.   Reiser, J.; Polu, K.R.; Möller, C.C.; Kenlan, P.; Altintas, M.M.; Wei, C.; Faul, C.; Herbert, S.; Villegas, I.;
505   Avila-Casado, C.; et al. TRPC6 is a glomerular slit diaphragm-associated channel required for normal renal
506   function. *Nat Genet* **2005**, *37*, 739–744, doi:10.1038/ng1592.

507   38.   Wang, Q.; Tian, X.; Wang, Y.; Wang, Y.; Li, J.; Zhao, T.; Li, P. Role of Transient Receptor Potential Canonical
508   Channel 6 (TRPC6) in Diabetic Kidney Disease by Regulating Podocyte Actin Cytoskeleton Rearrangement
509   Available online: https://www.hindawi.com/journals/jdr/2020/6897390/ (accessed on Aug 11, 2020).

510   39.   Soulet, F.; Bodineau, C.; Hooks, K.B.; Descarpentrie, J.; Alves, I.; Dubreuil, M.; Mouchard, A.; Eugenie, M.;
511   Hoepffner, J.-L.; López, J.J.; et al. ELA/APELA precursor cleaved by furin displays tumor suppressor
512   function in renal cell carcinoma through mTORC1 activation. *JCI Insight* **2020**, *5*,
513   doi:10.1172/jci.insight.129070.

514   40.   He, Z.; Thorrez, L.; Siegfried, G.; Meulemans, S.; Evrard, S.; Tejpar, S.; Khatib, A.-M.; Creemers*, J.W.M.
515   Differential Gene expression of furin knockout (KO) DLD1, HCA7 and HT29 colorectal cancer cells. GEO
516   Accession viewer Available online: https://www.ncbi.nlm.nih.gov/geo/query/acc.cgi?acc=GSE130969
517   (accessed on Apr 26, 2020).

518   41.   Khatib, A.-M.; Lahlil, R.; Scamuffa, N.; Akimenko, M.-A.; Ernest, S.; Lomri, A.; Lalou, C.; Seidah, N.G.;
519   Villoutreix, B.O.; Calvo, F.; et al. Zebrafish ProVEGF-C expression, proteolytic processing and inhibitory
520   effect of unprocessed ProVEGF-C during fin regeneration. *PLoS ONE* **2010**, *5*, e11438,
521   doi:10.1371/journal.pone.0011438.

522   42.   Siegfried, G.; Basak, A.; Prichett-Pejic, W.; Scamuffa, N.; Ma, L.; Benjannet, S.; Veinot, J.P.; Calvo, F.; Seidah,
523   N.; Khatib, A.-M. Regulation of the stepwise proteolytic cleavage and secretion of PDGF-B by the
524   proprotein convertases. *Oncogene* **2005**, *24*, 6925–6935, doi:10.1038/sj.onc.1208838.

525   43.   Zbidi, H.; Jardin, I.; Woodard, G.E.; Lopez, J.J.; Berna-Erro, A.; Salido, G.M.; Rosado, J.A. STIM1 and STIM2
526   Are Located in the Acidic Ca2+ Stores and Associates with Orai1 upon Depletion of the Acidic Stores in
527   Human Platelets. *J Biol Chem* **2011**, *286*, 12257–12270, doi:10.1074/jbc.M110.190694.

528   44.   Sanchez-Collado, J.; Lopez, J.J.; Jardin, I.; Camello, P.J.; Falcon, D.; Regodon, S.; Salido, G.M.; Smani, T.;
529   Rosado, J.A. Adenylyl Cyclase Type 8 Overexpression Impairs Phosphorylation-Dependent Orai1
530   Inactivation and Promotes Migration in MDA-MB-231 Breast Cancer Cells. *Cancers (Basel)* **2019**, *11*,
531   doi:10.3390/cancers11111624.
532   45.   Villoutreix, B.O.; Khatib, A.-M.; Cheng, Y.; Miteva, M.A.; Maréchal, X.; Vidal, J.; Reboud-Ravaux, M.
533   Blockade of the malignant phenotype by β-subunit selective noncovalent inhibition of immuno- and
534   constitutive proteasomes. *Oncotarget* **2017**, *8*, 10437–10449, doi:10.18632/oncotarget.14428.

535